Hindawi Publishing Corporation
Shock and Vibration
Volume 2016, Article ID 4028583, 7 pages
http://dx.doi.org/10.1155/2016/4028583

Research Article

Nonlinear Model of Vibrating Screen to Determine Permissible Spring Deterioration for Proper Separation

Cristian G. Rodriguez, Manuel A. Moncada, Emilio E. Dufeu, and Mario I. Razeto

Department of Mechanical Engineering, University of Concepcion, Edmundo Larenas 219, 4070409 Concepcion, Chile

Correspondence should be addressed to Cristian G. Rodriguez; cristian.rodriguez@udec.cl

Received 4 March 2016; Revised 2 August 2016; Accepted 8 August 2016

Academic Editor: Samuel da Silva

Springs of vibrating screens are prone to fatigue induced failure because they operate in a heavy duty environment, with abrasive dust and under heavy cyclic loads. If a spring breaks, the stiffness at supporting positions changes, and therefore the amplitude of motion and the static and dynamic angular inclination of deck motion also change. This change in the amplitude and in the inclination of motion produces a reduction in separation efficiency. Available models are useful to determine motion under nominal operating conditions when angular displacement is not significant. However in practice there is significant angular motion during startup, during shutdown, or under off-design operating conditions. In this article, a two-dimensional three-degree-of-freedom nonlinear model that considers significant angular motion and damping is developed. The proposed model allows the prediction of vibrating screen behavior when there is a reduction in spring stiffness. Making use of this model for an actual vibrating screen in operation in industry has permitted determining a limit for spring's failure before separation efficiency is affected. This information is of practical value for operation and maintenance staff helping to determine whether or not it is necessary to change springs, and hence optimizing stoppage time.

1. Introduction

Vibrating screens are important machines used to separate granulated ore materials based on particle size. In copper industry, the most used vibrating screens are of linear motion and with horizontal, sloped, or multisloped (banana) screen. Most of vibrating screens in copper industry are supported at four positions of the vibrating screen deck, and at each of these supporting positions there are two or more steel coil springs (depending on vibrating screen size there may be more supporting positions and springs). The springs of vibrating screens are prone to fail due to fatigue because they operate continuously in a heavy duty environment, with abrasive dust and under heavy cyclic loads.

If a spring in one supporting position breaks, then the stiffness of the supporting position decreases. If the stiffness decreases, then the amplitude of motion and the static and dynamic angular inclination of deck motion are expected to change in comparison to those expected at design operating conditions. A change in amplitude motion of 15% could produce a loss of separation efficiency of 5% [1]. A change in the angular inclination of deck motion produces a change in separation efficiency; for example, there are cases where the efficiency is 86% at design operating conditions and for a change of 2° in angle the separation efficiency drops to 55% [2, 3]. Xiao and Tong [4] show a drop of separation efficiency from 55% to 35% with a change of only 1°. The exact loss of efficiency due to amplitude or inclination deviation depends on the specific vibrating screen and the ore material characteristics. In order to ensure separation efficiency, the vibrating screen vendor provides a range of admissible amplitude and angle deviation for deck motion to operate. The proper amplitude and angle are checked during commissioning making measurements with accelerometers located at particular positions of vibrating screen deck.

In order to assure operation under design conditions (at a high separation efficiency), the evaluation of amplitude and angle of inclination due to spring condition would allow limiting spring deterioration. To be able to determine amplitude and angle of inclination due to spring condition

from vibration measurements, it is necessary to have a model able to predict how the deck will move when all springs are working at design conditions and how it will move when there is a loss of stiffness due to deteriorated springs.

Models of vibrating screens in literature are focused on separation [4–10], particles motion [11, 12], and failures in deck structure [13, 14]. Regarding vibrating screen motion, He and Liu [15] developed a three-degree-of-freedom linear model of a vibrating screen supported at two positions with equal stiffness for a circular motion vibrating screen. This model assumes stationary motion and a phase relationship between force and vibration of 0° in horizontal and vertical motion. With this assumption, a phase relationship of 90° between horizontal and vertical displacement is imposed, and the movement of vibrating screen center of mass results in an ellipse or a circle with a vertical or horizontal principal axis with no inclination. Liu et al. [16] developed a linear model of a vibrating screen supported in four different positions with different stiffness under a vertical force. This model did not consider the possibility of lateral motion of vibrating screen deck. They simulate supporting positions with loose of stiffness but because of model formulation they obtain a change in amplitude of the vertical displacement of the center of mass but movement could not change its inclination. Liu et al. [17] considered a linear model similar to He and Liu [15] but with a quadruple exciter mechanism. He and Liu [15], Liu et al. [16], and Liu et al. [17] consider no damping in their models. L. I. Slepyan and V. I. Slepyan [18] considered a linear model with damping and a tensile force for a linear motion vibrating screen with equal stiffness in all supporting positions. These linear models assume that angular motion of vibrating screen deck is low ($\sin\theta \approx \theta$ and $\cos\theta \approx 1$) and are useful for determining motion under nominal operating conditions because angular displacement is not significant but are not able to predict deck motion during the startup, during shutdown, or under off-design operating conditions such as the loss of stiffness in supporting positions. In practice, there is significant angular motion that occurs in vibrating screens during startup, during shutdown, and under off-design operating conditions.

In this article, a two-dimensional three-degree-of-freedom nonlinear model that considers significant angular motion and damping is developed in order to predict and evaluate the vibrating screen motion during startup, during shutdown, and under stationary operation conditions with deteriorated springs. The model simulates different deterioration levels of springs in order to determine its effect on amplitude and inclination of deck motion. The simulation is performed considering empty screen and full load. Empty screen is simulated because, after commissioning, the vibrating screen is tested empty in order to verify adequate amplitude and angle of inclination of motion. Full load is simulated because it is the normal operating condition and it is also the condition where springs operate under higher dynamic forces. With this simulation, it is possible to predict a range for acceptable spring deterioration in order to maintain proper motion to achieve an adequate separation efficiency. Finally, the model is compared with field measurements taken from a vibrating screen in use at a copper mine.

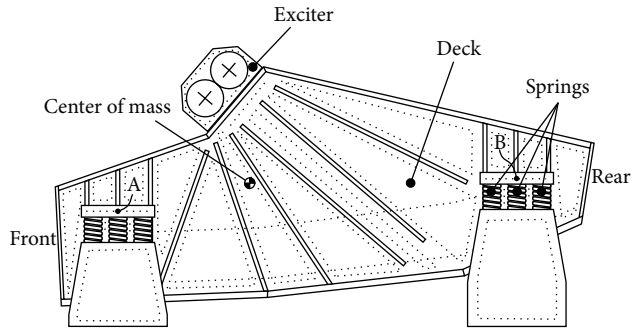

Figure 1: Vibrating screen.

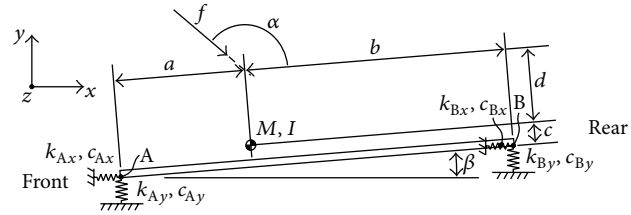

Figure 2: Model geometry.

2. The Model

In linear motion vibrating screens, motion is obtained by the action of a linear dynamic force produced by one or more exciter mechanisms. The linear force in the exciter mechanism is obtained by pairs of unbalanced masses mounted in pairs of different shafts that rotate at the same velocity but in different directions. Figure 1 shows a schematic of a vibrating screen with the exciter mechanism at the top of the deck.

The deck is supported by springs. Figure 2 shows the model of vibrating screen considered in this study, where M is the mass of the vibrating screen when in operation; I is the moment of inertia of the center of mass of the vibrating screen with respect to z-axis; k_{Ax}, k_{Ay}, k_{Bx}, and k_{By} are the stiffness of springs in horizontal and vertical directions in front and rear positions, respectively; c_{Ax}, c_{Ay}, c_{Bx}, and c_{By} are the damping of springs in horizontal and vertical directions in front and rear positions, respectively; f is the force due to the rotation of the unbalanced masses which is equal to $nm\omega^2 r \sin\omega t$, where n is the number of unbalanced masses, m the unbalanced mass, ω the rotating speed, and r the distance from the axis of rotation to the unbalance mass. The line AB is the line that connects the middle point of supporting position at the front (A) with the middle point of supporting position at the rear (B); a and b are the distances measured on the line AB between the front supporting position and the center of mass and between the center of mass and the rear supporting position, respectively; c is the distance from the center of mass to the line AB; d is the distance from the center of mass to the point that connects the projection of the line that defines the distance from the center of mass to the line AB, with the projection of the line where the excitation force f is acting; α is the angle of inclination of the force in relation to line AB; and β is the angle of inclination of line

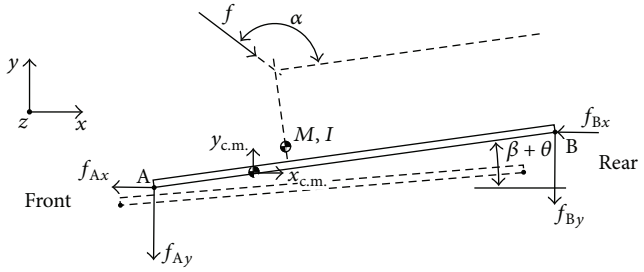

Figure 3: Model forces.

AB. To determine the equations of motion, it is assumed that the vibrating screen deck center of mass moves a distance $x_{c.m.}$ in the horizontal direction and a distance $y_{c.m.}$ in the vertical direction and that the screen rotates an angle θ (see Figure 3). With these considerations, the displacements x_A, y_A, x_B, and y_B at supporting positions are obtained as follows (see Figure 3)

$$\begin{aligned}
x_A &= x + \cos\theta\left[-a\cos\beta + c\sin\beta\right] \\
&\quad + \sin\beta\left[a\sin\beta + c\cos\beta\right] + a\cos\beta - c\sin\beta \\
y_A &= y + \cos\theta\left[-c\cos\beta - a\sin\beta\right] \\
&\quad + \sin\theta\left[c\sin\beta - a\cos\beta\right] + c\cos\beta + a\sin\beta \\
x_B &= x + \cos\theta\left[c\sin\beta + b\cos\beta\right] \\
&\quad + \sin\theta\left[c\cos\beta - b\sin\beta\right] - c\sin\beta - b\cos\beta \\
y_B &= y + \cos\theta\left[-c\cos\beta + b\sin\beta\right] \\
&\quad + \sin\theta\left[c\sin\beta + b\cos\beta\right] + c\cos\beta - b\sin\beta.
\end{aligned} \tag{1}$$

And consequently, the velocity of these positions is obtained as follows:

$$\begin{aligned}
\dot{x}_A &= \dot{x} - \dot{\theta}\sin\theta\left[-a\cos\beta + c\sin\beta\right] \\
&\quad + \dot{\theta}\cos\theta\left[a\sin\beta + c\cos\beta\right] \\
\dot{y}_A &= \dot{y} - \dot{\theta}\sin\theta\left[-c\cos\beta - a\sin\beta\right] \\
&\quad + \dot{\theta}\cos\theta\left[c\sin\beta - a\cos\beta\right] \\
\dot{x}_B &= \dot{x} - \dot{\theta}\sin\theta\left[c\sin\beta + b\cos\beta\right] \\
&\quad + \dot{\theta}\cos\theta\left[c\cos\beta - b\sin\beta\right] \\
\dot{y}_B &= \dot{y} - \dot{\theta}\sin\theta\left[-c\cos\beta + b\sin\beta\right] \\
&\quad + \dot{\theta}\cos\theta\left[c\sin\beta + b\cos\beta\right].
\end{aligned} \tag{2}$$

In linear models, the terms $\cos\theta$ and $\sin\theta$ are linearized, which is accurate when angular displacements are not significant. Nevertheless, these angular displacements are significant when the vibrating screen is operating during startup, during shutdown, or with deteriorated springs. To be able to predict the behavior under significant angular displacements, the equations of motion are as follows:

$$\begin{aligned}
&M\ddot{x} + \dot{x}\left[c_{Ax} + c_{Bx}\right] - \dot{\theta}\sin\theta\left[c_{Ax}\left(-a\cos\beta + c\sin\beta\right)\right. \\
&\quad \left. + c_{Bx}\left(c\sin\beta + b\cos\beta\right)\right] + \dot{\theta} \\
&\quad \cdot \cos\theta\left[c_{Ax}\left(a\sin\beta + c\cos\beta\right)\right. \\
&\quad \left. + c_{Bx}\left(c\cos\beta - b\sin\beta\right)\right] + x\left[k_{Ax} + k_{Bx}\right] \\
&\quad + \cos\theta\left[k_{Ax}\left(c\sin\beta - a\cos\beta\right)\right. \\
&\quad \left. + k_{Bx}\left(c\sin\beta - b\cos\beta\right)\right] \\
&\quad + \sin\theta\left[k_{Ax}\left(c\cos\beta + a\sin\beta\right)\right. \\
&\quad \left. + k_{Bx}\left(c\cos\beta - b\sin\beta\right)\right] + k_{Ax}\left(a\cos\beta - c\sin\beta\right) \\
&\quad + k_{Bx}\left(-c\sin\beta - b\sin\beta\right) = F \\
&\quad \cdot \sin\omega t\left[\cos\theta\cos\left(\alpha + \beta\right) - \sin\theta\sin\left(\alpha + \beta\right)\right] \\
&M\ddot{y} + \dot{y}\left[c_{Ay} + c_{By}\right] - \dot{\theta}\sin\theta\left[c_{Ay}\left(-c\cos\beta - a\sin\beta\right)\right. \\
&\quad \left. + c_{By}\left(-c\cos\beta + b\sin\beta\right)\right] + \dot{\theta}\cos\theta\left[c_{Ay}\left(c\sin\beta\right.\right. \\
&\quad \left.\left. - a\cos\beta\right) + c_{By}\left(c\sin\beta - b\cos\beta\right)\right] + y\left[k_{Ay} + k_{By}\right] \\
&\quad + \cos\theta\left[k_{Ay}\left(-c\cos\beta - a\sin\beta\right) + k_{By}\left(-c\cos\beta\right.\right. \\
&\quad \left.\left. + b\sin\beta\right)\right] + \sin\theta\left[k_{Ay}\left(c\sin\beta - a\cos\beta\right)\right. \\
&\quad \left. + k_{By}\left(c\sin\beta + b\cos\beta\right)\right] + k_{Ay}\left(c\cos\beta + a\sin\beta\right) \\
&\quad + k_{By}\left(c\cos\beta - b\sin\beta\right) = F\sin\omega t\left[\cos\theta\sin\left(\alpha + \beta\right)\right. \\
&\quad \left. + \sin\theta\cos\left(\alpha + \beta\right)\right] \\
&I\ddot{\theta} + \dot{\theta}\sin\theta\cos\theta \\
&\quad \cdot \left\{c_{Ay}\left[\left(c\sin\beta - a\cos\beta\right)\left(-a\sin\beta - c\cos\beta\right)\right.\right. \\
&\quad \left. + \left(-c\cos\beta - a\sin\beta\right)\left(a\cos\beta - c\sin\beta\right)\right] \\
&\quad - c_{By}\left[\left(c\sin\beta + b\cos\beta\right)\left(-c\cos\beta - b\sin\beta\right)\right. \\
&\quad \left. - \left(c\cos\beta + b\sin\beta\right)\left(-c\sin\beta + b\cos\beta\right)\right] \\
&\quad - c_{Ax}\left[\left(a\sin\beta + c\cos\beta\right)\left(c\sin\beta - a\cos\beta\right)\right. \\
&\quad \left. - \left(a\cos\beta + c\sin\beta\right)\left(c\cos\beta + a\sin\beta\right)\right] \\
&\quad + c_{Bx}\left[\left(c\cos\beta - b\sin\beta\right)\left(c\sin\beta + b\cos\beta\right)\right. \\
&\quad \left.\left. + \left(c\sin\beta - b\cos\beta\right)\left(-c\cos\beta + b\sin\beta\right)\right]\right\} + \dot{\theta} \\
&\quad \cdot \cos^2\theta\left\{c_{Ay}\left[c\sin\beta - a\cos\beta\right]\left[a\cos\beta - c\sin\beta\right]\right. \\
&\quad - c_{By}\left[c\sin\beta + b\cos\beta\right]\left[-c\sin\beta + b\cos\beta\right] \\
&\quad - c_{Ax}\left[c\sin\beta + a\cos\beta\right]\left[c\cos\beta + a\sin\beta\right] \\
&\quad \left. + c_{Bx}\left[c\cos\beta - b\sin\beta\right]\left[-c\cos\beta + b\sin\beta\right]\right\} + \dot{\theta}
\end{aligned}$$

$$
\begin{aligned}
&\cdot \sin^2\theta \left\{c_{Ay}\left[-c\cos\beta - a\sin\beta\right]\left[-a\sin\beta - c\cos\beta\right]\right.\\
&- c_{By}\left[-c\cos\beta + b\sin\beta\right]\left[-c\cos\beta - b\sin\beta\right]\\
&- c_{Ax}\left[-a\cos\beta + c\sin\beta\right]\left[c\sin\beta - a\cos\beta\right]\\
&\left.+ c_{Bx}\left[c\sin\beta + b\cos\beta\right]\left[c\sin\beta + b\cos\beta\right]\right\} - \dot{x}\\
&\cdot \cos\theta\left[-c_{Ax}\left(c\cos\beta + a\sin\beta\right)\right.\\
&\left.+ c_{Bx}\left(-c\cos\beta + b\cos\beta\right)\right] - \dot{x}\\
&\cdot \sin\theta\left[-c_{Ax}\left(c\sin\beta - a\cos\beta\right)\right.\\
&\left.+ c_{Bx}\left(c\sin\beta + b\cos\beta\right)\right] - \dot{y}\\
&\cdot \cos\theta\left[c_{Ay}\left(a\cos\beta - c\sin\beta\right)\right.\\
&\left.- c_{By}\left(-c\sin\beta + b\cos\beta\right)\right] - \dot{y}\\
&\cdot \sin\theta\left[c_{Ay}\left(-a\sin\beta - c\cos\beta\right)\right.\\
&\left.- c_{By}\left(-c\cos\beta - b\sin\beta\right)\right] + x\\
&\cdot \cos\theta\left[k_{Ax}\left(a\sin\beta + c\cos\beta\right)\right.\\
&\left.+ k_{Bx}\left(b\sin\beta - c\cos\beta\right)\right] + x\\
&\cdot \sin\theta\left[k_{Ax}\left(a\cos\beta - c\sin\beta\right)\right.\\
&\left.+ k_{Bx}\left(b\cos\beta + c\sin\beta\right)\right] + y\\
&\cdot \cos\theta\left[k_{Ay}\left(a\cos\beta - c\sin\beta\right)\right.\\
&\left.+ k_{By}\left(b\cos\beta + c\sin\beta\right)\right] + y\\
&\cdot \sin\theta\left[k_{Ay}\left(-a\sin\beta - c\cos\beta\right)\right.\\
&\left.+ k_{By}\left(-b\sin\beta + c\cos\beta\right)\right] + \cos 2\theta\\
&\cdot \left\{k_{Ax}\left[ac\left(-\cos^2\beta + \sin^2\beta\right)\right.\right.\\
&\left.+ \left(c^2 - a^2\right)\sin\beta\cos\beta\right] + k_{Ay}\left[ac\left(-\cos^2\beta + \sin^2\beta\right)\right.\\
&\left.+ \left(c^2 - a^2\right)\sin\beta\cos\beta\right] + k_{Bx}\left[bc\left(-\cos^2\beta + \sin^2\beta\right)\right.\\
&\left.+ \left(-c^2 + b^2\right)\sin\beta\cos\beta\right]\\
&+ k_{By}\left[bc\left(-\cos^2\beta + \sin^2\beta\right)\right.\\
&\left.\left.+ \left(-c^2 + b^2\right)\sin\beta\cos\beta\right]\right\} + \cos\theta\sin\theta\\
&\cdot \left\{k_{Ax}\left[4ac\cos\beta\sin\beta + \left(-c^2 + a^2\right)\sin^2\beta\right.\right.\\
&\left.+ \left(c^2 - a^2\right)\cos^2\beta\right] + k_{Ay}\left[4ac\cos\beta\sin\beta\right.\\
&\left.+ \left(-c^2 + a^2\right)\sin^2\beta + \left(c^2 - a^2\right)\cos^2\beta\right]\\
&+ k_{Bx}\left[4bc\cos\beta\sin\beta + \left(-c^2 + b^2\right)\sin^2\beta\right.\\
&\left.+ \left(c^2 - b^2\right)\cos^2\beta\right] + k_{By}\left[4bc\cos\beta\sin\beta\right.\\
&\left.+ \left(-c^2 + b^2\right)\sin^2\beta + \left(c^2 - b^2\right)\cos^2\beta\right]\right\} + \cos\theta\\
&\cdot \left\{k_{Ax}\left[ac\left(\cos^2\beta - \sin^2\beta\right)\right.\right.\\
&\left.+ \left(-c^2 + a^2\right)\sin\beta\cos\beta\right] + k_{Ay}\left[ac\left(\cos^2\beta - \sin^2\beta\right)\right.\\
&\left.+ \left(-c^2 + a^2\right)\sin\beta\cos\beta\right] + k_{Bx}\left[bc\left(\cos^2\beta - \sin^2\beta\right)\right.\\
&\left.+ \left(c^2 - b^2\right)\sin\beta\cos\beta\right] + k_{By}\left[bc\left(\cos^2\beta - \sin^2\beta\right)\right.\\
&\left.\left.+ \left(c^2 - b^2\right)\sin\beta\cos\beta\right]\right\} + \sin\theta\left\{k_{Ax}\left[a\cos\beta\right.\right.\\
&\left.- c\sin\beta\right]^2 + k_{Ay}\left[-2ac\sin\beta\cos\beta - c^2\cos^2\beta\right.\\
&\left.- a^2\sin^2\beta\right] + k_{Bx}\left[-2bc\sin\beta\cos\beta - c^2\sin^2\beta\right.\\
&\left.- cb^2\cos^2\beta\right] + k_{By}\left[-2bc\sin\beta\cos\beta + c^2\cos^2\beta\right.\\
&\left.\left.- b^2\sin^2\beta\right]\right\} = -F\sin\omega t\cdot d.
\end{aligned}
\tag{3}
$$

These three equations correspond to a second-order nonlinear system of equations, which can be reduced in a series of first-order differential equations solved making use of Runge-Kutta method with variable time step.

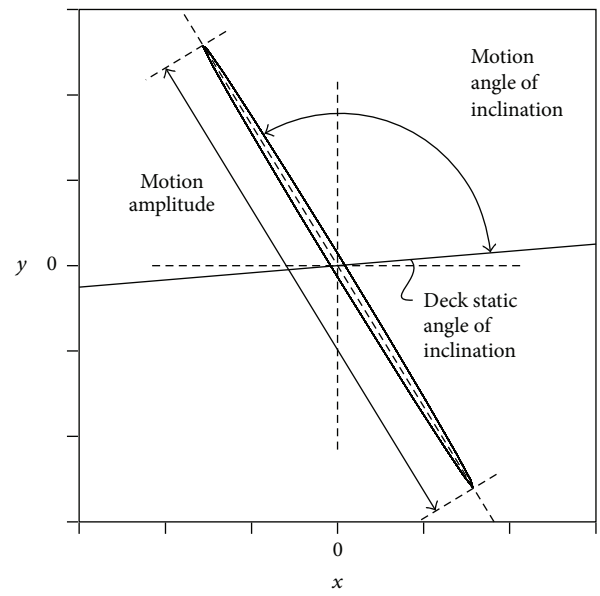

Figure 4: Motion characteristics measured in linear vibrating screens.

3. Vibrating Screen Motion

The motion measured on the linear vibrating screen is mainly defined by two variables: the amplitude and the angle of inclination of motion as shown in Figure 4. In this section, the behavior of these two variables under different stiffness at supporting positions is analyzed.

As stated above, the present simulations make use of the data obtained from a vibrating screen in use at a copper mine

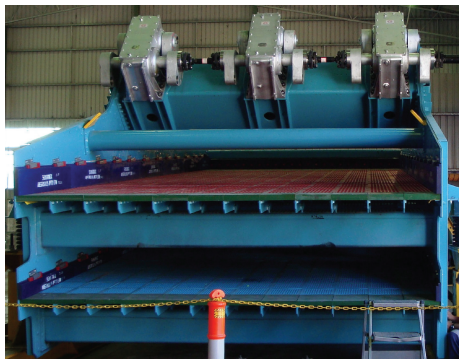

Figure 5: Simulated vibrating screen, front view.

(Figure 5). The characteristics of the vibrating screen when operating without load are $a = 2054$ mm; $b = 3896$ mm; $c = 298$ mm; $d = 1372$ mm; $\beta = 4{,}8^{\circ}$; $\alpha = 135^{\circ}$; $k_{Ay} = k_{By} = 4992000$ N/m; $k_{Ax} = k_{Bx} = 2064000$ N/m; $M = 24468$ kg; $I = 622443$ kg m^2; $n = 6$; $m = 100$ kg; $\omega = 98{,}96$ rad/s; and $r = 0{,}225$ m.

The vibrating screen motion is obtained in the model after applying the excitation force f. To simulate startup of vibrating screen, the frequency of f is considered as variable from zero to nominal rotating speed. The rise of frequency from zero to nominal rotating conditions is considered as a normal for an induction motor startup. The amplitude of force f is determined by the unbalance force that is proportional to $134{,}4\,\omega^2$ N. Approximately 20 seconds after force f reaches nominal rotating speed, the stationary motion is obtained. This procedure is repeated for the nominal stiffness of springs and for all combinations from 100% to 10% of stiffness in decrements of 10% in front and rear supporting positions. With this, the motion of vibrating screen for 81 combinations of different stiffness in front and rear supporting positions is obtained. Figure 6 shows the motion obtained in the front supporting position, center of mass, and rear supporting position for no deterioration of springs, thus for 100% of nominal stiffness k_A and k_B.

Figure 6 shows the deviation in angle of inclination from the angle at design operating conditions for the center of mass. The same angle lines in Figure 7 are obtained after interpolating selected angles between obtained angles for the 81 simulations. Angle deviation at front and rear supporting positions behaves similarly and for that reason graphs for these positions are not shown. For all the cases simulated considering empty screen, the amplitude of motion changes between a −2,3% and a +0,9% which is below vendor limits for amplitude deviation and for that reason it is not shown in a graph.

After empty vibrating screen is simulated, the model is solved considering a full load of mineral. For this case, the position of the center of mass, total mass, and moment of inertia change from those considered for the case of empty vibrating screen simulation. The values used in simulations of full load operation of the vibrating screen are $a = 2917$ mm; $b = 3033$ mm; $c = 0$ mm; $d = 667$ mm; $M = 48497$ kg; and $I = 1156474$ kg m^2.

In Figure 8, the motions obtained in the front supporting position, center of mass, and rear supporting position for no deterioration of springs and full load are shown. Figure 9 shows the deviation of angle from the angle at design operating conditions. For all the simulated cases considering full load screen, the amplitude of motion changes between a −1,9% and a +0,0% which is below vendor limits for amplitude deviation, and for that reason it is not graphically shown herein. In Figure 9, the limit of operation indicated by the manufacturer ($\pm 2^{\circ}$) is depicted by a wider solid line. It can be observed that with these two curves a limit of stiffness can be defined in order to ensure that the loss of stiffness in the supporting positions has no influence in the proper operation of the vibrating screen.

In order to maintain separation efficiency, this model is capable of defining a limit for spring stiffness. It has been shown that adequate stiffness at supporting positions is important to maintain a proper operation of vibrating screen. It has also been observed that, for an actual vibrating screen, amplitude variations due to loss of stiffness are not significant with variations differing from −2,3% to +0,9%; this difference has negligible effect on separation efficiency; in practice when there are differences in the amplitude of motion, this is solved by modifying unbalance masses configuration. From the values obtained from Figure 9 it can be observed that, in this vibrating screen, half of stiffness in the front supporting position (46% k_A) and almost a third of stiffness in the rear supporting position (38% k_B) can be allowed. Therefore, maintenance can be performed after one of each two or one of each three springs is broken at the front and the rear supporting positions, respectively. Because in the simulated vibrating screen each supporting position has eight springs in parallel, then the separation efficiency will not be significantly affected before 54% and 62% of springs are broken at the front and the rear supporting positions, respectively, which leads to a maximum of four springs broken in each supporting position. The number of springs to break before maintenance will depend on the particular vibrating screen characteristics and therefore should be calculated for each particular case.

4. Conclusions

Available models of vibrating screen motion are useful to predict its behavior under nominal operation conditions.

The model proposed in this article can predict behavior of vibrating screen motion under nominal operating conditions as well as under significant angular displacement: transient conditions, resonance conditions, and different stiffness at supporting positions.

These novel capabilities of the proposed model allow the prediction of vibrating screen behavior when there is damage in spring stiffness and, therefore, allow evaluating whether it is necessary to replace springs or not in order to achieve an adequate separation efficiency, or to reduce overhaul time, thus increasing vibrating screen availability.

Making use of this model for an actual vibrating screen has permitted determining a limit for spring's stiffness reduction before separation efficiency is affected. For the simulated vibrating screen, the minimum allowed stiffness is 46% and

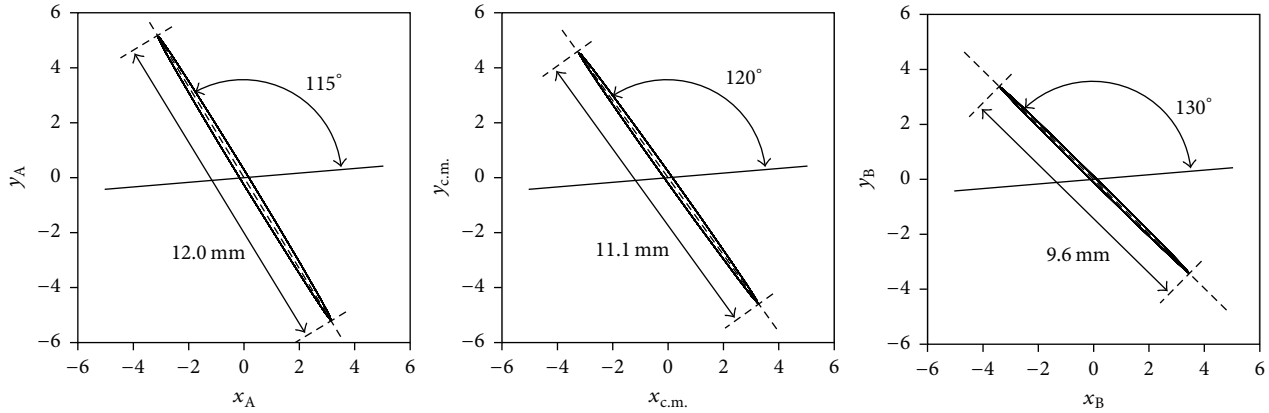

Figure 6: Movement in mm front supporting position (A), center of mass (c.m.), and rear supporting position (B) for nominal operating conditions, empty screen.

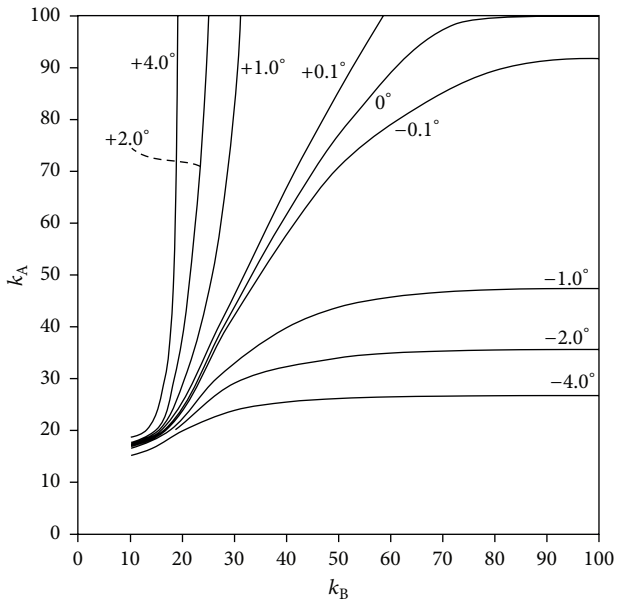

Figure 7: Angle deviation in movement of center of mass for different stiffness in front and rear supporting positions as percentage of nominal stiffness, empty screen.

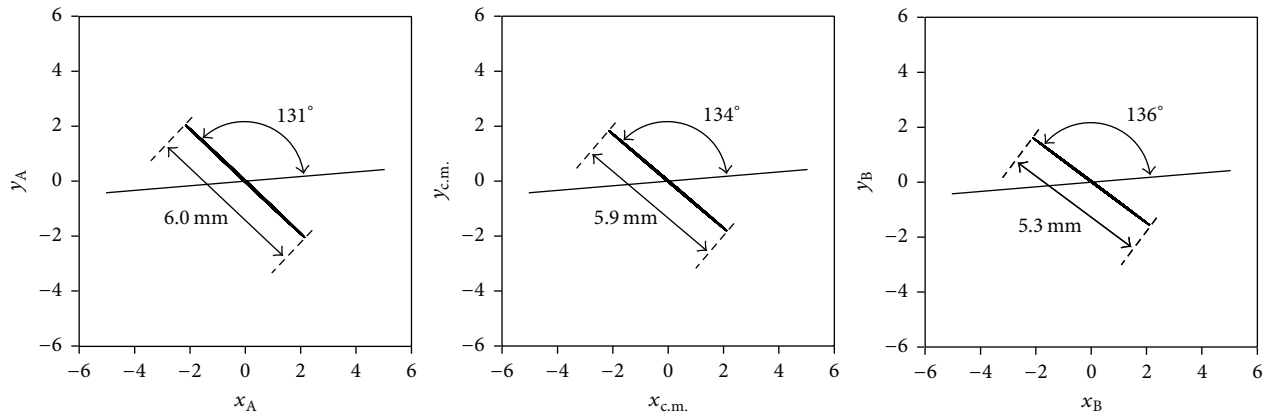

Figure 8: Movement in front supporting position (A), center of mass (c.m.), and rear supporting position (B) for nominal operating conditions, full load.

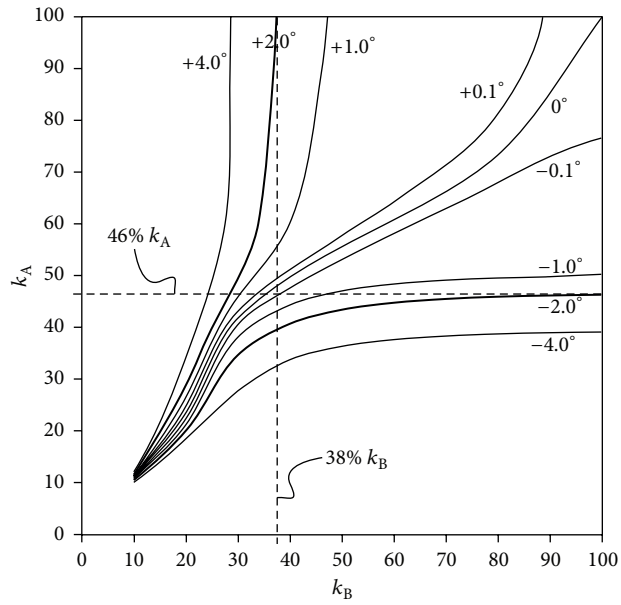

Figure 9: Angle deviation in the movement of the center of mass, full load.

38% of nominal stiffness in the front and rear supporting position, respectively. Because each supporting position has eight springs in parallel, then the failure of four springs can be allowed in each supporting position.

This information is of practical value for operation and maintenance staff helping to determine whether or not it is necessary to change springs, and hence optimizing stoppage time.

Additional Points

Highlights. (i) A two-dimensional three-degree-of-freedom nonlinear model is developed. (ii) The model is used to evaluate motion under off-design operating conditions. (iii) A limit for springs failure is determined before separation efficiency is affected. (iv) The model allows evaluating whether it is necessary to replace springs or not.

Competing Interests

The authors declare that there is no conflict of interests regarding the publication of this paper.

References

[1] L. Zhao, Y. Zhao, C. Liu, J. Li, and H. Dong, "Simulation of the screening process on a circularly vibrating screen using 3D-DEM," *Mining Science and Technology*, vol. 21, no. 5, pp. 677–680, 2011.

[2] E. G. Kelly, *Introduction to Mineral Processing*, John Wiley & Sons, New York, NY, USA, 1982.

[3] B. A. Wills, *Wills' Mineral Processing Technology: An Introduction to the Practical Aspects of Ore Treatment and Mineral Recovery*, Butterworth-Heinemann, Oxford, UK, 7th edition, 2006.

[4] J. Xiao and X. Tong, "Particle stratification and penetration of a linear vibrating screen by the discrete element method," *International Journal of Mining Science and Technology*, vol. 22, no. 3, pp. 357–362, 2012.

[5] P. W. Cleary, M. D. Sinnott, and R. D. Morrison, "Separation performance of double deck banana screens—part 1: flow and separation for different accelerations," *Minerals Engineering*, vol. 22, no. 14, pp. 1218–1229, 2009.

[6] P. W. Cleary, M. D. Sinnott, and R. D. Morrison, "Separation performance of double deck banana screens—part 2: quantitative predictions," *Minerals Engineering*, vol. 22, no. 14, pp. 1230–1244, 2009.

[7] I. M. Cotabarren, J. Rossit, V. Bucalá, and J. Piña, "Modeling of an industrial vibrating double-deck screen of a urea granulation circuit," *Industrial and Engineering Chemistry Research*, vol. 48, no. 6, pp. 3187–3196, 2009.

[8] G. Wang and X. Tong, "Screening efficiency and screen length of a linear vibrating screen using DEM 3D simulation," *Mining Science and Technology*, vol. 21, no. 3, pp. 451–455, 2011.

[9] M. Trumic and N. Magdalinovic, "New model of screening kinetics," *Minerals Engineering*, vol. 24, no. 1, pp. 42–49, 2011.

[10] J. Xiao and X. Tong, "Characteristics and efficiency of a new vibrating screen with a swing trace," *Particuology*, vol. 11, no. 5, pp. 601–606, 2013.

[11] K. J. Dong, A. B. Yu, and I. Brake, "DEM simulation of particle flow on a multi-deck banana screen," *Minerals Engineering*, vol. 22, no. 11, pp. 910–920, 2009.

[12] L. Zhao, C. Liu, and J. Yan, "A virtual experiment showing single particle motion on a linearly vibrating screen-deck," *Mining Science and Technology (China)*, vol. 20, no. 2, pp. 276–280, 2010.

[13] Y.-M. Zhao, C.-S. Liu, X.-M. He, C.-Y. Zhang, Y.-B. Wang, and Z.-T. Ren, "Dynamic design theory and application of large vibrating screen," *Procedia Earth and Planetary Science*, vol. 1, no. 1, pp. 776–784, 2009, Proceedings of the 6th International Conference on Mining Science & Technology.

[14] Z. Tang, Z. Yin, T. Han, X. Sun, and L. Zhang, "Research on dynamic characteristics of elliptical vibrating screen," in *Proceedings of the International Conference on Mechanic Automation and Control Engineering (MACE '10)*, pp. 2366–2369, IEEE, Wuhan, China, June 2010.

[15] X.-M. He and C.-S. Liu, "Dynamics and screening characteristics of a vibrating screen with variable elliptical trace," *Mining Science and Technology (China)*, vol. 19, no. 4, pp. 508–513, 2009.

[16] C. Liu, L. Peng, and F. Li, "Survey of signal processing methods and research on vibrating screen fault diagnosis," in *Proceedings of the 2nd International Conference on Mechanic Automation and Control Engineering (MACE '11)*, pp. 1709–1712, IEEE, Hohhot, China, July 2011.

[17] C.-S. Liu, S.-M. Zhang, H.-P. Zhou et al., "Dynamic analysis and simulation of four-axis forced synchronizing banana vibrating screen of variable linear trajectory," *Journal of Central South University*, vol. 19, no. 6, pp. 1530–1536, 2012.

[18] L. I. Slepyan and V. I. Slepyan, "Coupled mode parametric resonance in a vibrating screen model," *Mechanical Systems and Signal Processing*, vol. 43, no. 1-2, pp. 295–304, 2014.